The Journal of Engineering

Research Article

IET Journals
The Institution of Engineering and Technology

18 band ANSI S1.11 filter bank based on interpolated finite impulse response technique for hearing aids

eISSN 2051-3305
Received on 25th July 2019
Accepted on 23rd March 2020
E-First on 8th September 2020
doi: 10.1049/joe.2019.1009
www.ietdl.org

Deepu S.P.[1] ✉, *Ramesh Kini M.*[1], *Sumam David S.*[1]

[1]*Department of Electronics and Communication Engineering, National Institute of Technology Karnataka, Surathkal, Mangalore 575025, India*

✉ *E-mail: deepusp123@gmail.com*

Abstract: A low complexity interpolated finite impulse response (IFIR) based 18 band ANSI S1.11 1/3 octave digital filter bank for hearing aid is proposed and implemented using 65 nm UMC technology in this study. ANSI S1.11 specifications for 1/3 octave Class-2 filters are chosen as design criteria in the proposed method. The strict requirements at lower bands make the hardware implementation of ANSI S1.11 filter bank complex and difficult in a power critical application like hearing aid. In the proposed technique, the maximum margin available in the filter specifications is utilised in both upper and lower band edge specifications to reduce the filter order. IFIR technique was used to reduce the computations at lower bands which can be implemented in hardware efficiently without altering the sampling frequency of the input signal. Compared to other recent architectures, >50% reduction in total number of filter coefficients is achieved and the group delay is kept <10 ms. Hardware implementation of the algorithm was done using 65 nm standard cell libraries and tested the outputs with NAL-NL2 gain prescriptions. The matching errors are within ± 1.5 dB and the core power consumption was obtained as 0.37 mW.

1 Introduction

According to the World Health Organisation, around 50% of young people aged between 12–35 years are at risk of hearing loss due to excessive exposure to loud sounds including music from personal audio devices [1]. Fundamental blocks present in the digital signal processing part of a basic digital hearing aid are filter bank (FB), dynamic range compression (DRC), noise reduction (NR) and acoustic feedback cancellation (FBC). Out of these, FB and DRC perform the basic functionality of a hearing aid that is loudness compensation and signal compression while NR and FBC are optional blocks used for further signal enhancement. Hearing aid being a real-time application powered by a small battery, the circuit complexity should be as low as possible meeting the required delay constraint. At the same time, the algorithm should provide enough frequency resolution to keep the matching error between the prescribed gain and initial fitting as small as possible.

Finite impulse response (FIR) filters are preferred over infinite impulse response (IIR) filters because of their linear phase characteristics and inherent stability. Uniform or non-uniform FB architecture can be used and initially, uniform structures were used in hearing aids. Lunner and Hellgren [2] proposed an eight band uniform FB based on interpolated FIR technique [3]. McAllister *et al.* [4] used frequency sampling technique and the FB was based on a comb filter which combines with a bank of 167 resonators spaced at 50 Hz intervals over the frequency range 0–8.3 kHz. A frequency-domain implementation of an oversampled, weighted overlap-add (WOLA) FB is described in [5]. In WOLA architecture, a single prototype filter was replicated to 32 equal bands by DFT modulation. Advantages of the multidimensional logarithmic number system for hardware implementation were utilised in [6] and designed an 8-channel uniform FB structure using Kaiser window based parallel FIR filters.

In uniform FB, a large number of bands are required to get sufficient frequency resolution to match the audiograms at lower frequencies compared to non-uniform architectures. Research interest shifted to non-uniform architectures for hearing aid application in recent years. A frequency response masking technique was proposed by Lian and Wei [7] for hearing aids. It is a symmetric non-uniform FB which gives higher resolution at lower and higher frequencies, but lesser resolution at middle bands, hence the matching error is high at middle frequencies. A hardware implementation of the FRM technique using a 16 band non-uniform FB is proposed in [8]. Even though the matching errors for the algorithm were calculated directly for the audiogram instead of any gain prescription, the maximum matching error is high in some cases since the algorithm was based on the FRM technique, which differs from frequency domain characteristics of cochlea significantly. A technique based on frequency warping is proposed by Lai *et al.* [9], in which uniform cosine modulated FB is modified using all pass transform to obtain non-uniform structure. It would be difficult to meet the specifications in hardware because of its recursive and complicated structure and can cause problems with stability. A low complexity multirate ANSI S1.11 18 band FB was proposed in [10], which uses three prototype filters to define the upper octave. Remaining bands are derived from it using multirate technique. The algorithm suffers from a high group delay (GD) which is not acceptable for hearing aid application. Further modifications to multirate ANSI S1.11 18 band structure are proposed by Liu *et al.* [11] and Yang *et al.* [12]. Liu and coworkers [10] reduced the GD to 10 ms by restricting the down sampling factor to four for the lower nine bands. The upper nine bands were designed the same as in. Yang *et al.* [12], derived the whole 18 bands from a single prototype filter by using fractional sampling rates. Both these architectures are not following ANSI S1.11 specifications and are running at multiple sampling rates for different bands which will make the synthesis part complex in hardware implementation and can cause problems while incorporating other multi-band algorithms like NR and DRC.

A three-channel variable band IIR FB was proposed for hearing aid application by Deng *et al.* in [13]. The design was based on a variable low pass, variable bandpass and variable high pass digital filters. The three filters were obtained from a Chebyshev type-1 low pass filter using frequency transformations. The algorithm suffers from high audiogram matching error along with the disadvantages of being IIR. The hardware implementation of the system may also be difficult considering the requirement of adjusting the bandwidth of each band according to each audiogram.

In this study, we propose a comparatively simple architecture that satisfies ANSI S1.11 specifications with a lesser number of filter coefficients without altering the sampling rate. The band edge frequencies are carefully designed by utilising the maximum margin available to meet the ANSI specifications which reduce the prototype filter's order considerably. The entire FB is implemented on hardware and the hardware design was tested using NAL-NL2

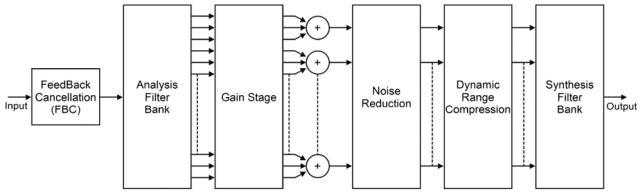

Fig. 1 *Basic signal processing blocks present in a digital hearing aid*

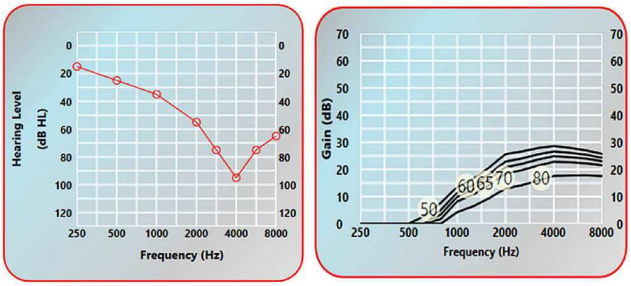

Fig. 2 *Sample audiogram and its corresponding NAL-NL2 prescription gains*

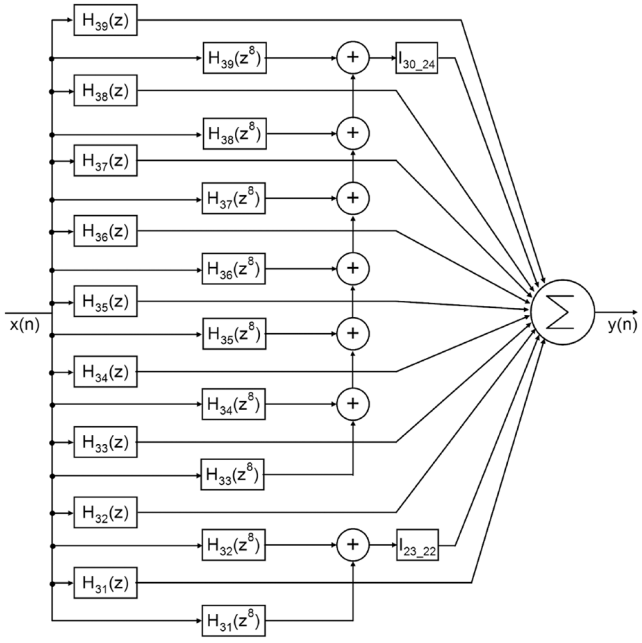

Fig. 3 *Proposed FB architecture*

prescriptions for different audiograms, which is not available in the literature for ANSI S1.11 specifications to our knowledge. The background of ANSI S1.11 fractional filter specifications and basic hearing aid working is discussed in Section 2. The proposed architecture is explained in Section 3. Details of hardware implementation are described in Section 4. Simulation results and performance analysis are given in Section 5.

2 Background

Basic signal processing components present in a hearing aid chip are shown in Fig. 1. In hearing aid fitting, the insertion gains obtained from various prescription formulas are applied to different bands to fit the audiogram. DRC algorithm is used to compress the signal levels, which cross a particular threshold after the application of gain to protect the residual hearing. NR and DRC can be applied as single channel or multichannel. Multichannel DRC [14] and multiband NR [15, 16] give better performance over single channel processing.

An audiologist uses various prescription formulas to fit the audiogram. Most commonly used ones are National Acoustics Laboratory-Non Linear1 (NAL-NL1), NAL-NL2 [17, 18] and desired sensation level input/output formula [19]. These methods prescribe the insertion gains in terms of 1/3 octave bands from 160 Hz to 8 kHz, which closely match the spectral characteristics of the cochlea. A sample audiogram and its NAL-NL2 prescription are shown in Fig. 2. ANSI S1.11 standard defines the specifications for 1/3 octave band pass filters from 25 Hz to 20 kHz [20]. 18 bands from 157 Hz to 8 kHz are chosen which covers the entire audiogram frequency spectrum. The center frequency, f_{m_n}, of n^{th} band is defined as

$$f_{m\_n} = (G^{(n-30)/b})(f_r) \tag{1}$$

where G is the octave ratio which is 2 for base-2 systems, n is the frequency band number and f_r is the reference frequency which is 1 kHz. For 1/3 octave b is 3. The band numbers corresponding to 157 Hz is 22 and that of 8 kHz is 39. The lower and upper pass band edges of the filters are defined as

$$f_{p1\_n} = (G^{-1/(2b)})(f_{m\_n}) \tag{2}$$

$$f_{p2\_n} = (G^{+1/(2b)})(f_{m\_n}) \tag{3}$$

the pass band for each 1/3 octave is defined as $f_{p2\_n} - f_{p1\_n}$. The maximum pass band ripple (δ_1) for Class-2 filters is specified as ± 0.5 dB for each band and minimum stop band attenuation (δ_2) is 60 dB. The stop band edge frequencies for 60 dB attenuation is specified as

$$f_{s1\_n} = 0.184 f_{m\_n} \tag{4}$$

$$f_{s2\_n} = 5.435 f_{m\_n} \tag{5}$$

3 Proposed algorithm

The architecture of the proposed FB is shown in Fig. 3. Parks-McClellan (PM) algorithm is followed for prototype filter design [21]. The order of the filter in PM algorithm is given by

$$P \simeq \frac{-10\log_{10}(\delta_1\delta_2) - 13}{2.43 B_{\text{TW}}} \tag{6}$$

where $B_{\text{TW}} = \min(B_{\text{TW}_1}, B_{\text{TW}_2})$. B_{TW_1} and B_{TW_2} are transition bandwidths $(f_{p1} - f_{s1})$ and $(f_{s2} - f_{p2})$, respectively. Equation (6) shows that increasing the minimum transition bandwidth will decrease the order of the filter. According to ANSI S1.11 Class-2 specifications, the band edge frequencies for H_{22}, i.e. f_{s1_22}, f_{p1_22}, f_{p2_22} and f_{s2_22} are 29, 140, 177 and 853 Hz, respectively. Modifying the band edge frequencies according to minimum of transition bandwidths which is 111 Hz yields new specification as 29, 140, 177 and 288 Hz. The direct FIR implementation for the above specification gives an order of 430 which will result in 216 multiplications per sample for band 22 alone and will cause a GD of ~9 ms for a sampling frequency of 24 kHz.

Considering the upper band, i.e. H_{39}, the ANSI S1.11 Class-2 specifications for the band edge frequencies are 1472, 7127, 8980 and 43,478 Hz. Taking the minimum of transition bandwidths, the band edge frequencies will get modified to 1472, 7127, 8980 and 14,635 Hz. To meet this specification, a sampling frequency of 29,270 Hz is required to satisfy the Nyquist criteria, which is high for hearing aids. In hearing aids, the frequency spectrum is highly restricted by transducer frequency characteristics, generally in the range of 5 kHz for both microphones as well as receivers. Audiograms are recorded for a frequency spectrum of 160 Hz to 8 kHz and hence a sampling frequency <16 kHz is required. We opted for a sampling frequency of 24 kHz as frequencies beyond 8 kHz are perceptually insignificant in practical hearing aids. It also facilitates a comparison of the performance of the architecture with other ANSI S1.11 based FBs [9–12] which also use a sampling frequency of 24 kHz. So the specifications are modified to the maximum margin possible, i.e. 4107, 7127, 8980 and 12,000 Hz, which gave a filter order of 16. We opted for critical sampling

Table 1 Band edge specifications for filters H_{39}, H_{31} and H_{22} to meet the required design criteria for the 18-band structure

Filter	f_{s1}, Hz	f_{p1}, Hz	f_{p2}, Hz	f_{s2}, Hz
H_{39}	4107	7127	8980	**12,000**
H_{31}	229	1123	1414	2308
H_{22}	**29**	140	177	288

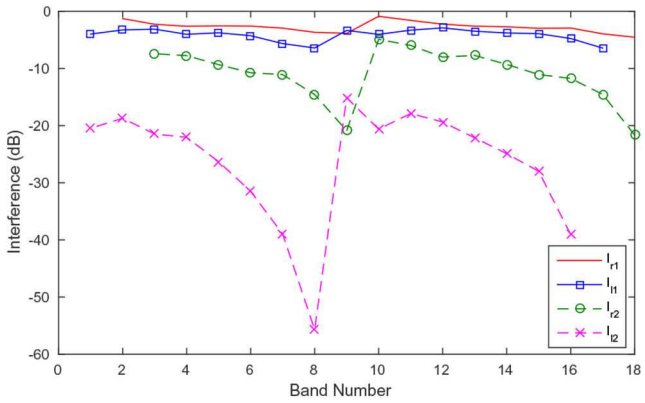

Fig. 4 *Plot of Interband Interference from neighbouring bands*

considering the fact that in practical hearing aids, the frequencies beyond 8 kHz do not matter much. This analysis shows that the lowest stop band edge is decided by the ANSI S1.11 specifications, i.e.f_{s1_22} and highest stop band edge is decided by the sampling frequency, i.e. f_{s2_39} which is still within the required ANSI specifications.

In the proposed architecture, interpolated FIR (IFIR) technique [22] is used to reduce the computational complexity. The upper nine prototype filters (H_{39}–H_{31}) were designed separately using PM algorithm and interpolated by a factor of 8 to obtain the lower 9 filters ($H_{30} - H_{22}$). ANSI S1.11 requirements are used to design filter H_{31} so that it will meet the specification for lowest band, H_{22}. Therefore, the band edge specifications for H_{31} are 229, 1123, 1414 and 2308 Hz. Based on the above design criteria, the required band edge specifications for filters H_{39}, H_{31} and H_{22} are as given in Table 1. The upper stop band edges for filters H_{32}–H_{38} are computed using a linear interpolation between the upper stop band edges of H_{31} (f_{s2_31}) and H_{39} (f_{s2_39}) in octave scale as given below

$$y_{s2\_n} = r(f_{m\_n} - f_{m\_39}) + y_{s2\_39} \tag{7}$$

where

$$r = \frac{y_{s2\_31} - y_{s2\_39}}{f_{m\_31} - f_{m\_39}} \tag{8}$$

$$y_{s2\_n} = G^{f_{s2\_n}/f_{m\_n}} \tag{9}$$

where f_{s2_n} is the upper stop band edge and f_{m_n} is the centre frequency of n^{th} band. Calculated band edge frequencies and its corresponding orders for filters f_{39}–f_{31} are given in Table 2.

This new band structure will distribute the inter-band interference almost uniformly among all the 18 bands since the band edges are linearly varying from H_{31} to H_{39} in a logarithmic scale and satisfy the ANSI S1.11 specifications with reduced filter order. Fig. 4 shows the plot of inter-band interference from the first and second neighbouring bands to each filter. I_{r1} is interference from the first neighbouring band from the right side, I_{r2} is the interference from the second neighbouring band from the right side, I_{l1} is the interference from the first neighbouring band from left side and I_{l2} is the interference from the second neighbouring band from left side. It can be observed that the interference from the first neighbouring bands is almost uniformly distributed among all the bands except for the case of interference between bands 9 and 10. Since band 10 is derived from band 18 instead of band 9, there is a comparable difference in slope in the interference plot between bands 9 and 10. Interference from the second neighbouring bands is <−10 dB in most of the cases, which is negligible compared to first neighbouring band interference.

Table 2 Prototype filter specifications

Band number, n	Band edge frequencies, Hz $[f_{s1}\ f_{p1}\ f_{p2}\ f_{s2}]$	Filter order
39	[4107 7127 8980 12000]	16
38	[2698 5657 7127 10087]	16
37	[1805 4490 5657 8342]	18
36	[1230 3564 4490 6824]	20
35	[853 2829 3564 5540]	24
34	[600 2245 2829 4474]	28
33	[429 1782 2245 3597]	36
32	[312 1414 1782 2884]	44
31	[229 1123 1414 2308]	54

The GD of an IFIR combination can be calculated as

$$\text{GD} = \frac{N_{\text{a}} * L + N_{\text{i}}}{2f_{\text{s}}} \tag{10}$$

where L is the interpolation factor, N_{a} and N_{i} represent orders of analysis and interpolation filters, respectively, and f_{s} is the sampling frequency.

Since the interpolation factor is high, the constraints on image cancellation filter specification become high. Here transition bandwidth of interpolation filter is decided by f_{p2_30} of H_{30} and f_{s1_22} of first image of H_{22}, which gives an order of 118 for the low pass filter. It will adversely affect the GD as well as total multiplications per sample of the entire system. To reduce the GD, two interpolation filters are used instead of one, which will relax the band edge requirements. For example, let the lower 9 band filters be grouped into two as H_{30_28} and H_{27_22} and two low pass filters I_{30_28} and I_{27_22} be used to cancel out the image frequencies of H_{30_28} and H_{27_22}. Then the band edge requirements of I_{30_28} is decided by f_{p2_30} of H_{30} and f_{s1_28} of first image of H_{28} which is higher than those of H_{22}, so the order of I_{30_28} is obtained as 80. Similarly the band edge requirements of I_{27_22} is decided by f_{p2_27} of H_{27} which is lesser than that of H_{30} and f_{s1_22} of first image of H_{22} and the order of I_{27_22} is obtained as 50. Now the maximum GD of the entire structure is decided by the maximum of GDs introduced by the combinations of (H_{30_28}&I_{30_28}) and (H_{27_22}&I_{27_22}), which is 4.67 and 10.04 ms, respectively. Table 3 shows the exploration results of the order of interpolation filters for all the combinations of the analysis filters in groups of two and their respective GDs.

It can be observed that filter pair (H_{30_24} H_{23_22}) gives the minimum GD of 9.75 ms with a slight increase in the total number of multiplications required to 75 for interpolation filters.

4 Hardware implementation

The hardware realisation structure of the proposed FB is shown in Fig. 5. The architecture contains a total of 20 filters with odd tap length. The co-efficient symmetry property of the filters is used to reduce the number of multiplications. Table 4 shows the filter orders and the corresponding number of multiplications required for each filter.

The entire system was implemented using 16 bit fixed point arithmetic. The prescribed gains G_{xy}, obtained from the NAL-NL2

formula, are applied to the input signal as it passes through each filter. These gains are stored in programmable registers. Separate input ports are provided to load the gain values and input data. A five bit address is needed to choose between different gains.

After interpolation, the tap length of filter H_{22} becomes 433, which requires the maximum number of delay registers among all 18 bands. This delay line can be shared between the 18 analysis filters. Two separate delay lines are required for interpolation filters I_{30_24} and I_{23_22} of lengths 111 and 37, respectively. Nineteen buffer registers are needed to synchronise filters from H_{39} to H_{31} as shown in Fig. 5. Similarly, 80 buffer registers are needed to synchronise filters from H_{30} to H_{24} and 48 buffers are needed between filters H_{23} and H_{22}. The maximum GD of the proposed architecture is due to the combination of filter H_{22} and the interpolation filter I_{23_22}. So 207 and 35 buffer registers are needed to synchronise the upper nine bands and the output of interpolation filter I_{30_24}, respectively. So the proposed FB architecture requires a total of 581 data line registers and 389 synchronisation buffers to satisfy the linear phase condition. The entire FB needs to be synchronised according to three delay lines as shown in Fig. 6. That is, H_{23} and H_{22} should be synchronised according to the delay line of 433 before passing to I_{23_22}. Filters from H_{24} to H_{30} should be synchronised before passing

Table 3 Interpolation filter order exploration

Pair No.	Filter pair	Interpolation filter order pair	GD Pair	#MPY
P1	H_{30} H_{29_22}	54 74	3.79 10.54	66
P2	H_{30_29} H_{28_22}	66 58	4.04 10.21	64
P3	H_{30_28} H_{27_22}	80 50	4.67 10.04	67
P4	H_{30_27} H_{26_22}	90 44	5.21 9.92	69
P5	H_{30_26} H_{25_22}	98 40	6.04 9.83	71
P6	H_{30_25} H_{24_22}	106 38	6.88 9.79	74
P7	H_{30_24} H_{23_22}	110 36	8.29 9.75	75
P8	H_{30_23} H_{22}	114 36	9.70 9.75	77
P9	H_{30_22}	118	11.46	60

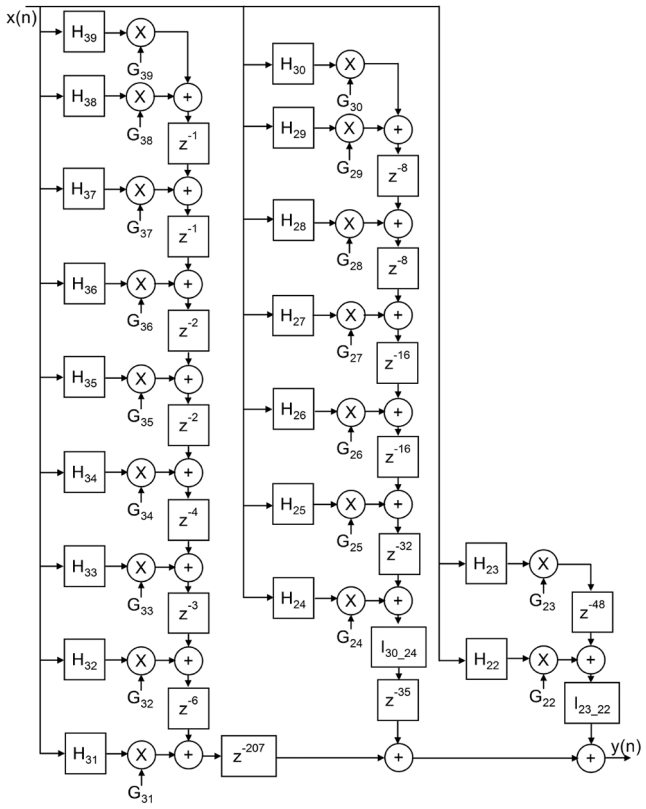

Fig. 5 *Hardware realisation structure of the proposed FB algorithm*

Table 4 Filter tap lengths and number of multiplications required for each filter

Filter	H_{39}	H_{38}	H_{37}	H_{36}	H_{35}	H_{34}	H_{33}	H_{32}	H_{31}	I_{30_24}
Tap length	17	17	19	21	25	29	37	43	55	111
#Multiplications	9	9	10	11	13	15	19	22	28	56

Filter	H_{30}	H_{29}	H_{28}	H_{27}	H_{26}	H_{25}	H_{24}	H_{23}	H_{22}	I_{23_22}
Tap length	129	129	145	161	193	225	289	337	433	37
#Multiplications	9	9	10	11	13	15	19	22	28	19

the combined output to the delay line for I_{30_24}. Finally, the combination of filters from H_{31} to H_{39} and the output from I_{30_24} should be synchronised with the output of I_{23_22}.

A multi-MAC based design was followed for the implementation of the proposed algorithm which is preferred for low power consumption [11]. Sampling frequency was chosen as 24 kHz. The entire FB was designed using 30 MAC units with a clock frequency of 384 kHz. Various possibilities for the number of MAC units are explored as given in Table 5. Total number of multiplications per sample for the proposed architecture is 347. If a single MAC unit is used for performing all the multiplications, a clock frequency of 8.328 MHz will be required. Increased clock frequency will cause higher switching power dissipation. If we use one MAC per filter, i.e. 20 MAC units for 20 different filters, then I_{30_24} alone requires 56 multiplications per MAC, which will require a minimum clock frequency of 1.344 MHz. After exploring the different possible options, 30 MAC units were selected with 15 multiplications per MAC, considering the number of stall cycles and the ratio of logic to sequential cells.

Using a clock of 384 kHz requires ten extra MAC units to complete the entire filtering. Four MAC units are required for I_{30_24} and 2 MAC units per filter are required for I_{23_22}, H_{22}, H_{23}, H_{24}, H_{31}, H_{32} and H_{33}, since the number of multiplications needed are >15 in these filters. For example, the interpolating filter, I_{30_24} needs four MAC units to perform one complete convolution as shown in Fig. 7. N represents the order of the filter and k is the count value from 0 to 15. From Fig. 7, it can be observed that the longest flop to flop path constitutes only one multiplier, two adders and two multiplexers. Since I_{30_24} requires 56 multiplications per sample (MPY), 14 multiplications per MAC will be enough to complete one convolution operation which will result in 1 stall cycle per MAC. Outputs of all four MAC registers (*MAC30_241Reg* to *MAC30_244Reg*) are added once the count value reaches 14 and stored in the output register of filter I_{30_24}, which is *MAC30_24_Reg* as shown in the figure. Therefore, one extra cycle is needed to perform this final addition operation for the outputs of four different MAC units. In the case of filter I_{23_22}, only two accumulators are needed instead of four.

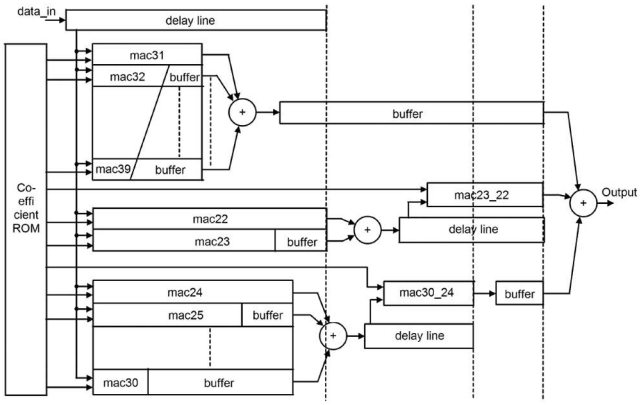

Fig. 6 *Synchronisation buffer structure of the proposed architecture*

5 Simulation results and discussion

All the filter coefficients were obtained using MATLAB® 2015.2 with Signal Processing toolbox. *firpm* function was used to design the prototype filters. Filter tap lengths were adjusted to next higher order where required, to make all the filters of type I, which will make the hardware implementation easier. Frequency response of the designed 18 band FB is shown in Fig. 8. According to ANSI S1.11 Class-2 filter specifications, the passband ripples should be within ±0.5 dB, which is important to keep the final audiogram matching error within ±1.5 dB. However, the inter-band interference from adjacent bands and the contribution of ripples from the interpolation filter can adversely affect the overall passband distortion from the desired specification. So a two-stage gain optimisation procedure was followed as given in [12] to reduce the effect of inter-band interference and the interpolation filter ripple contribution, to make the overall matching error within ±1.5 dB. During the first stage of gain optimisation, the average flat band error was kept within ±0.5 dB. This gain offset was added

Table 5 Operations per MAC and the required clock frequencies

No. of MAC units	Multiplications/MAC	Min. Clock Freq., MHz
1	347	8.328
2	272, 75	6.528
2	174	4.2
20	56	1.344
30	15	0.384
347	1	0.48

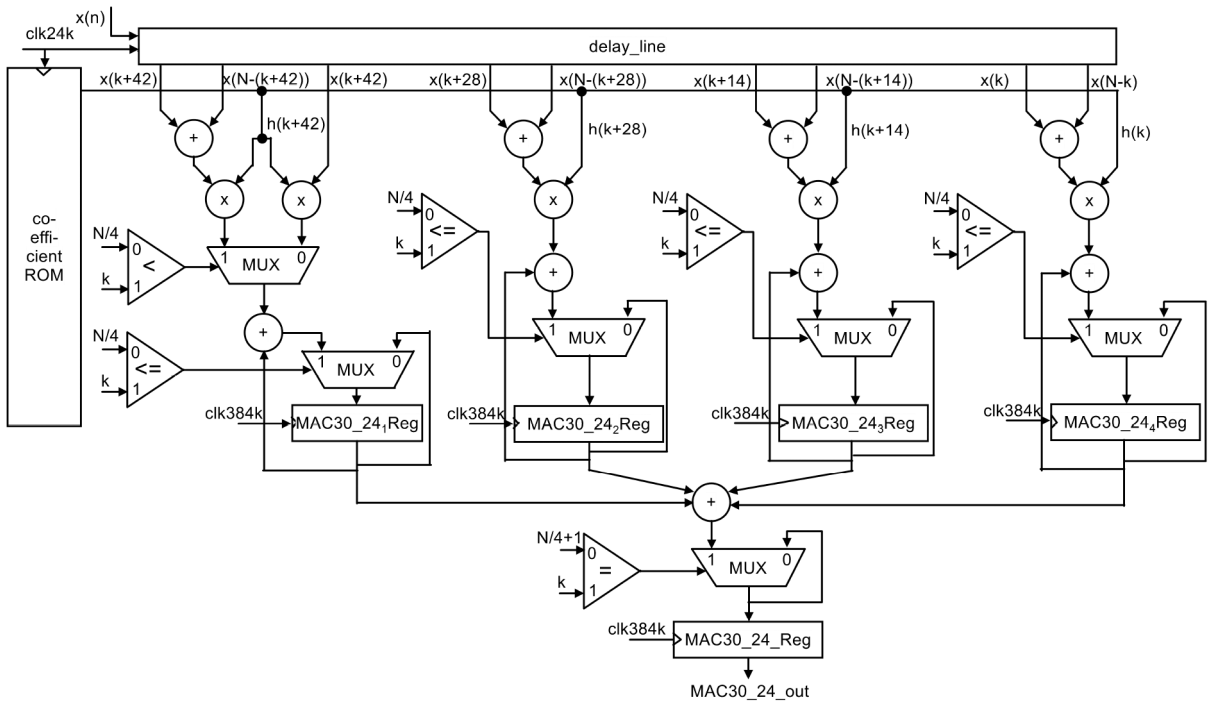

Fig. 7 *Hardware architecture of the multi MAC unit of filter I_{30_24}*

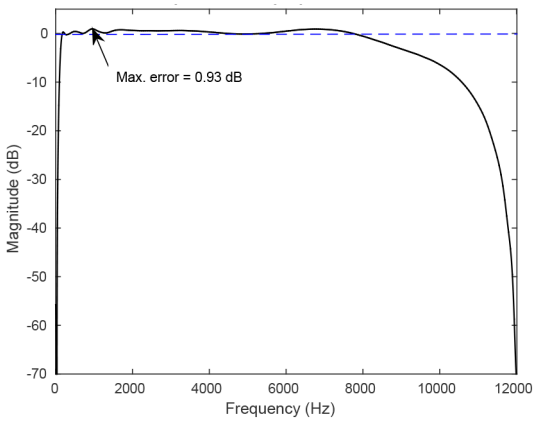

Fig. 9 *Flat band response of the FB*

to the prescribed gain and applied the same optimisation algorithm during the second stage after applying the fitting gain to keep the final fitting error $<\pm 1.5$ dB. The flat band response of the proposed FB is shown in Fig. 9.

5.1 Comparison with other architectures

A comparison with other architectures available in the literature is given in Table 6. Kuo *et al.* [10] introduced the use of ANSI S1.11 specifications for fractional octave FBs for hearing aid application. They used multirate architecture to reduce computational complexity. Three prototype filters were used to generate the entire FB along with interpolation and decimation filters. The design was satisfying the specifications with a lesser number of coefficients but the GD (78 ms) was high. Liu *et al.* [11] modified the architecture to meet the delay constraint of 10 ms by relaxing the ANSI specifications and constricting the downsampling factor to four. They used the same design as in [10] for upper three octaves and lower 3 octaves were designed with a restricted downsampling factor of 4. All the lower six filters were designed with the same order of 97, which is redundant considering the requirements for filters other than filter H_{22}. Yang *et al.* [12], further modified the architecture in such a way that the 18 bands are generated from a single prototype filter by fractional sub-sampling. This architecture is also a relaxed version of ANSI S1.11 specifications. In [12], every band is at a different sampling rate which is difficult to implement practically as other algorithms like DRC and NR are also to be implemented in hearing aids. The modifications to [10] in later publications were mainly focussed on lower 9 bands which were responsible for increased complexity and delay. The upper 9 bands specifications of [11, 12] were similar to [10].

In the proposed design, the complexity of the upper 9 bands was reduced by carefully stretching the design criteria to its maximum possible limits within ANSI S1.11 specifications and

Table 6 Comparison table

Reference	Type	No. of coefficients	Delay, ms
[10]	ANSI	91	78
[11]	Quasi ANSI	506	10
[23]	Quasi ANSI	451	13.58
[12]	Quasi ANSI	579	10
proposed	ANSI	212	9.75

derived the lower 9 band filters from them. This approach resulted in a large reduction in filter order required for upper 9 bands and an overall reduction in the total number of filter coefficients required for the 18 band filter structure. The design requires 212 coefficients, which is <50% of other architectures with similar GD. Another ANSI S1.11 architecture available in the literature is [9], which used a non-linear structure based on frequency warping and a combination of cosine modulation and all pass transform. The algorithm was not tested after hardware implementation. Lai's *et al.* also conclude that the architecture will cause phase distortion due to the IIR structure used in it. The linear phase requirement is important if FBC algorithms are to be incorporated in the hearing aid.

Considering the hardware implementations available in the literature for ANSI S1.11 specifications based architectures, [10, 11] have implemented only the analysis FB and not the synthesis FB. In [10], authors have given the hardware results for the analysis part, which requires fewer number of storage elements, but its synthesis part requires 3432 buffer registers to meet the linear phase requirement which is large. Moreover, different octaves are running at different sampling frequencies, which will require the generation of different clock frequencies. Handling clock domain crossing issues may become critical in hardware implementation when other complex signal enhancement algorithms like DRC and NR are to be added at different bands. The generation of the different clock frequencies will necessitate overhead logic as well. The synthesis will become complex as buffers of different bands at different frequencies will have to be synchronised even though the architecture has a regular structure. Similar problems can arise in [11] due to its multirate structure.

Comparing to the above two architectures, the proposed algorithm has the same sampling frequency for all the filters at the cost of a slight increase in the number of multiplications per sample. It is more practical to implement and easier to incorporate other signal enhancement algorithms without altering the sampling rate.

5.2 Hardware results

The entire architecture is implemented using Verilog Hardware Description Language, and synthesised, placed and routed with Cadence® Design tools using UMC 65 nm standard cell libraries.

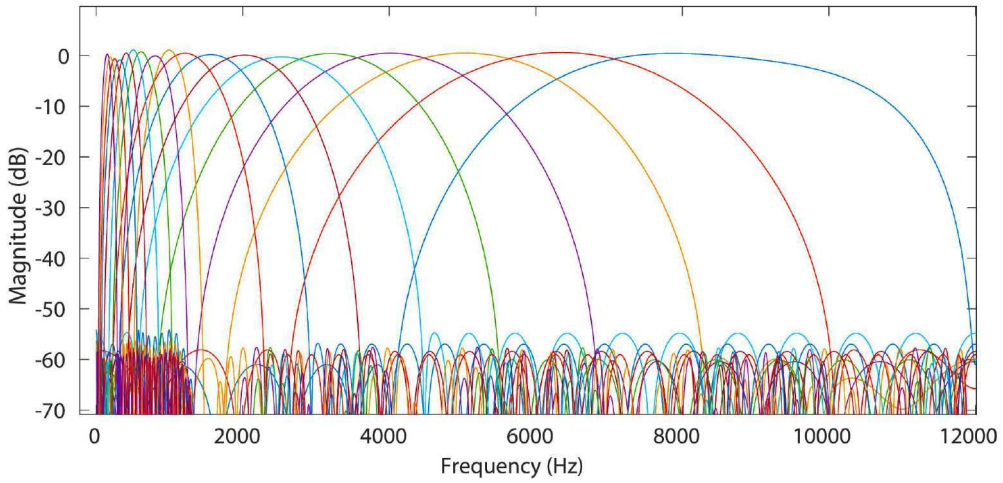

Fig. 8 *Frequency response of the FB*

Table 7 Quantisation error (dB)

Centre freq., Hz	160	200	250	315	400	500	630	800	1000	1250	1600	2000	2500	3150	4000	5000	6300	8000
audiogram2	0.1	0.118	0.054	0.05	0.074	0.083	0.093	0.063	0.07	0.087	0.073	0.075	0.085	0.086	0.081	0.08	0.076	0.079
audiogram3	0.108	0.118	0.061	0.054	0.077	0.086	0.095	0.067	0.072	0.094	0.077	0.079	0.081	0.086	0.083	0.081	0.081	0.082
audiogram4	0.104	0.115	0.057	0.054	0.076	0.087	0.089	0.071	0.076	0.093	0.077	0.078	0.076	0.088	0.088	0.085	0.079	0.082
audiogram5	0.113	0.122	0.074	0.062	0.079	0.083	0.101	0.072	0.074	0.094	0.079	0.079	0.08	0.085	0.082	0.082	0.08	0.082
audiogram6	0.111	0.121	0.086	0.079	0.066	0.076	0.101	0.061	0.071	0.095	0.078	0.08	0.081	0.085	0.083	0.082	0.08	0.083
audiogram7	0.106	0.112	0.052	0.042	0.084	0.09	0.086	0.073	0.082	0.094	0.081	0.078	0.082	0.087	0.087	0.087	0.084	0.085
audiogram8	0.109	0.119	0.066	0.062	0.078	0.089	0.093	0.073	0.08	0.097	0.082	0.082	0.083	0.089	0.086	0.085	0.083	0.086
audiogram9	0.11	0.119	0.061	0.052	0.081	0.092	0.091	0.075	0.08	0.095	0.081	0.08	0.082	0.089	0.088	0.086	0.083	0.086

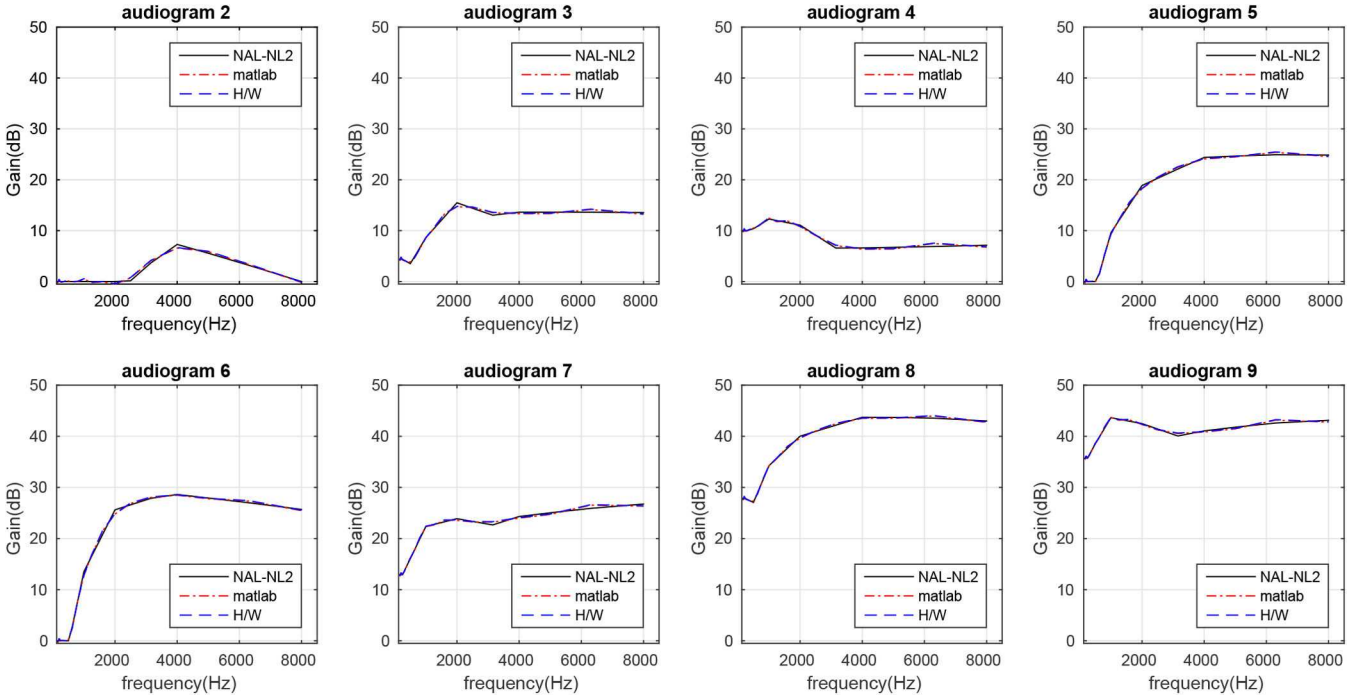

Fig. 10 *Gain matching results for NAL-NL2 prescriptions for different audiograms*

Table 8 Audiogram matching error

Audiogram	2	3	4	5	6	7	8	9
max. error, dB	0.641	0.710	0.672	0.553	0.758	0.715	0.499	0.654

Table 9 Power results

Power	FB with DRC, mW	FB without DRC, mW
internal	0.1598	0.1554
switching	0.2041	0.1930
leakage	0.0260	0.0253
total	0.3900	0.3737

Post layout core power analysis was done using Cadence Voltus^{TM} IC Power Integrity Solution with a maximum switching activity factor of one for typical parasitic corner.

Audiograms corresponding to most commonly found eight different hearing losses available in [24], are widely used in research related to audiogram fitting. The prescribed insertion gains for each audiogram were obtained from the NAL-NL2 formula for an input level of 50 dB. The gains were applied to the proposed FB implementation and matching error for each band for all the audiograms were obtained. The quantisation error was obtained by comparing the 16-bit hardware implementation results with the MATLAB double precision implementation of the proposed architecture. The quantisation error results are given in Table 7. It can be observed that the maximum quantisation error is 0.122 dB. The audiogram matching results are shown in Fig. 10. The maximum matching error for each audiogram is given in Table 8. The results show that the error is $<\pm 1$ dB in all the cases which is less than the audible difference of 1.5 dB. Audiogram 6, which is having a rapidly changing slope, has the maximum matching error.

Post implementation core power results are given in Table 9 for a supply voltage of 1.2 V. The FB architecture consumes a total power of 0.37 mW. The FB algorithm was combined with a single channel DRC [25] and tested with a sample audio file for flatband condition and without any compression applied. The input and reconstructed output waveforms are shown in Fig. 11. The FB with DRC consumes a power of 0.39 mW. In state of the art hearing aids, audio CODEC [26] and transducers [27] generally consume around 0.35 mW of power. To meet the minimum specification of <1 mW [28], for a digital hearing aid, the DSP part is having a power margin of around 0.65 mW in which, the FB consumes most of the power compared to other signal enhancing algorithms. The proposed algorithm consumes only around 60% of the available power margin with a standard implementation. Power consumption can be further reduced by applying various low power design techniques. The chip is having a die area of 0.81 mm^2 and 71,215 standard cells with 43.4% of logic cells, 55.1% sequential cells and 1.5% of inverters. To compare the power consumption, the entire algorithm was implemented using 2 MAC units, one for all the 18 analysis bands and one for both the interpolation filters, which requires a clock frequency of 6.528 MHz and the power consumption was obtained as 5.044 mW. It shows that multi MAC

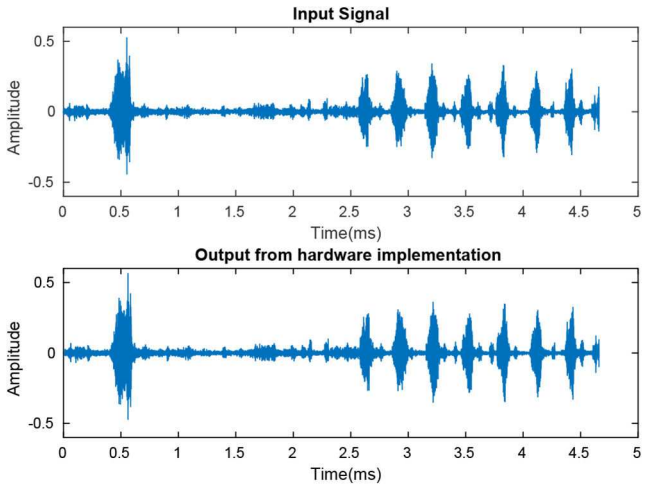

Fig. 11 *Sample audio output waveform from post-layout hardware simulation*

architecture with lesser multiplications per single MAC unit consumes less power.

6 Conclusion

In this study, a complexity-oriented architecture for ANSI S1.11 1/3 octave Class-2 FB for hearing aids is developed. A method to define band edge frequencies of each prototype filter to get minimum order which satisfies the required specifications is proposed. Hardware implementation of the algorithm was carried out using 65 nm standard cell libraries. The hardware output was tested with NAL-NL2 prescription for different audiograms and the maximum matching error was within the practical limit of ± 1.5 dB. The proposed architecture shows >50% reduction in the total number of filter coefficients required and <10 ms GD with practically applicable power consumption. Future work includes incorporating multiband NR algorithm and a multichannel compression algorithm to the proposed FB. Since the entire FB is running at the same sampling frequency, incorporating such algorithms will be easier compared to multirate architectures. The overall performance of the algorithm can be improved further by applying low power hardware implementation techniques. The number of MAC units required may be optimised with a better design space exploration and can change depending upon the filter structure. Developing a generalised solution to find the best possible number of MAC units can also be taken as a future work.

7 Acknowledgment

The authors thank the Ministry of Electronics and Information Technology (MeitY), Government of India and the Special Manpower Development Programme for Chips to System Design (SMDP-C2SD) for providing EDA tools support.

8 References

[1] World Health Organisation: 'Deafness and hearing loss', 15 March 2018. accessed 19 February 2019. https://www.who.int/news-room/fact-sheets/detail/deafness-and-hearing-loss

[2] Lunner, T., Hellgren, J.: 'A digital filterbank hearing aid-design, implementation and evaluation'. 1991 Int. Conf. on Acoustics, Speech, and Signal Processing, 1991. ICASSP-91, Toronto, Ontario, Canada, 1991, pp. 3661–3664

[3] Nielsen, L.S., Sparso, J.: 'Designing asynchronous circuits for low power: an IFIR filter bank for a digital hearing aid', *Proc. IEEE*, 1999, **87**, (2), pp. 268–281

[4] McAllister, H., Black, N., Waterman, N., *et al.*: 'Audiogram matching using frequency sampling filters'. Engineering in Medicine and Biology Society, 1994. Engineering Advances: New Opportunities for Biomedical Engineers. Proc. 16th Annual Int. Conf. of the IEEE, Baltimore, MD, USA, 1994, vol. 1, pp. 249–250

[5] Brennan, R., Schneider, T.: 'A flexible filterbank structure for extensive signal manipulations in digital hearing aids'. Proc. 1998 IEEE Int. Symp. on Circuits and Systems, 1998. ISCAS'98, Monterey, CA, USA, 1998, vol. 6, pp. 569–572

[6] Li, H., Jullien, G., Dimitrov, V., *et al.*: 'A 2-digit multidimensional logarithmic number system filterbank for a digital hearing aid architecture'. IEEE Int. Symp. on Circuits and Systems, 2002. ISCAS 2002, Phoenix-Scottsdale, AZ, USA, 2002, vol. 2, pp. I–II

[7] Lian, Y., Wei, Y.: 'A computationally efficient nonuniform FIR digital filter bank for hearing aids', *IEEE Trans. Circuits Syst. I, Regul. Pap.*, 2005, **52**, (12), pp. 2754–2762

[8] Wei, Y., Ma, T., Ho, B.K., *et al.*: 'The design of low-power 16-band nonuniform filter bank for hearing aids', *IEEE Trans. Biomed. Circuits Syst.*, 2019, **13**, (1), pp. 112–123

[9] Lai, S.C., Liu, C.H., Wang, L.Y., *et al.*: '11.25-ms group delay and low complexity algorithm design of 18-band quasi-ANSI S1.11 1/3 octave digital filter bank for hearing aids', *IEEE Trans. Circuits Syst. I, Regul. Pap.*, 2015, **62**, (6), pp. 1572–1581

[10] Kuo, Y.T., Lin, T.J., Li, Y.T., *et al.*: 'Design and implementation of low power ANSI S1.11 filter bank for digital hearing aids', *IEEE Trans. Circuits Syst. I, Regul. Pap.*, 2010, **57**, (7), pp. 1684–1696

[11] Liu, C.W., Chang, K.C., Chuang, M.H., *et al.*: '10-ms 18 band quasi-ANSI S1.11 1/3 octave filter bank for digital hearing aids', *IEEE Trans. Circuits Syst. I, Regul. Pap.*, 2013, **60**, (3), pp. 638–649

[12] Yang, C.Y., Liu, C.W., Jou, S.J.: 'A systematic ANSI S1.11 filter bank specification relaxation and its efficient multirate architecture for hearing aid systems', *IEEE/ACM Trans. Audio Speech Lang. Process.*, 2016, **24**, (8), pp. 1380–1392

[13] Deng, T.B.: 'Three-channel variable filter-bank for digital hearing aids', *IET Signal Process.*, 2010, **4**, (2), pp. 181–196

[14] Yund, E.W., Buckles, K.M.: 'Multichannel compression hearing aids: effect of number of channels on speech discrimination in noise', *J. Acoust. Soc. Am.*, 1995, **97**, (2), pp. 1206–1223

[15] Loizou, P.C.: '*Speech enhancement: theory and practice*' (CRC press, Florida, USA, 2007)

[16] Wei, C.W., Tsai, C.C., FanJiang, Y., *et al.*: 'Analysis and implementation of low-power perceptual multiband noise reduction for the hearing aids application', *IET Circuits Devices Syst.*, 2014, **8**, (6), pp. 516–525

[17] Byrne, D., Dillon, H., Ching, T., *et al.*: 'NAL-NL1 procedure for fitting nonlinear hearing aids: characteristics and comparisons with other procedures', *J. Am. Acad. Audiol.*, 2001, **12**, (1), pp. 37–51

[18] Keidser, G., Dillon, H., Flax, M., *et al.*: 'The NAL-NL2 prescription procedure', *Audiol. Res.*, 2011, **1**, (1), pp. 88–90

[19] Scollie, S., Seewald, R., Cornelisse, L., *et al.*: 'The desired sensation level multistage input/output algorithm', *Trends Amplif.*, 2005, **9**, (4), pp. 159–197

[20] 'Specifications for octave and fractional-octave-band analog and digital filters'. ANSI, 2004. S1.11

[21] Kaiser, J.F.: 'Nonrecursive digital filter design using the i-sinh window function'. Proc. 1974 IEEE Int. Symp. on Circuits & Systems, San Francisco DA, April 1974, pp. 20–23

[22] Vaidyanathan, P.P.: '*Multirate systems and filter banks*' (Pearson Education India, India, 1993)

[23] Lai, S.C., Liu, C.H., Wang, L.Y., *et al.*: '14-ms group delay and low complexity algorithm design of 18 band quasi-ANSI S1.11 1/3 octave filter bank for digital hearing aids'. 2014 Tenth Int. Conf. on Intelligent Information Hiding and Multimedia Signal Processing (IIH-MSP), Kitakyushu, Japan, 2014, pp. 81–84

[24] 'How to read your hearing test'. Available at http://www.earinfo.com/how-to-read-a-hearing-aid-test/common-audiograms

[25] Deepu, S.P., Sumam, D.S., Ramesh, K.M.: 'Estimation of attack time constant for dynamic range compressors in hearing aids'. 2016 IEEE Int. Conf. on Digital Signal Processing (DSP), Beijing, People's Republic of China 2016, pp. 20–24

[26] 'Aic111: 1.3-v micro power single channel codec'. Available at http://www.ti.com/product/AIC111/description

[27] 'Mems microphones, the future for hearing aids'. Available at https://www.analog.com/en/analog-dialogue/articles/mems-microphones-future-for-hearing-aids.html

[28] 'Guidelines for hearing aids and services for developing countries'. World Health Organisation, 2004